Constrained Constructive Optimization implementation
Reproducing Rudolph Karch paper

CLARA JAQUET
Paris-Est University
October 12, 2016

Abstract

This report aims to explain the CCO algorithm implementation in 2D, and its 3D extension. This algorithm has been detailed by Schreiner in 2D [3] and Karch in 3D [1]. Because the implementation principle is spread between several articles, we propose to summarize hereafter the whole implementation. Along the way, we provide our own interpretation of some finer details of the method, that leave room for variants.

The CCO algorithm combines computational fluid dynamics laws, network geometry and topology optimization to mimic vascular network growth.

Keywords: constrained constructive optimization, implementation

Contents

Introduction

Constrained Constructive Optimization (CCO) consists of growing a tree governed by minimizing a target function.

In Karch's method the tree is constrained into a growing convex perfusion volume, and the target function minimizes the total tree volume. Segments are added one by one and subjected to both local optimization (single bifurcation scale) and global optimization (tree scale). The local optimization is based on Kamiya's work [2], whereas the global tree optimization has been implemented first by Schreiner in 2D [3].

1 Global tree optimization

Initialization of the method requires as input some physiological parameters, the number of terminal segments to reach, and a randomized starting point.

The CCO algorithm is introduced with the organigram in figure 1.

Each loop of the algorithm determines a new segment to be added onto the tree. Figure 2 provides an example of the result of the first three loops. The perfusion territory is slightly increased before each new added segment, to simulate tissue growth concomitant with vascular growth. A random location is picked under some constraints (geometrical and physiological), to use it as a candidate for segment extremity. Its connection is tested with neighbor segments, producing a bifurcation under topological, structural and functional constraints. Due to mechanical laws, each connection also induces a specific adjustment of all existing segment diameters. The optimal connection is then selected among all connections as the one minimizing a target function (the minimal volume of the total tree).

1.1 Assumptions and boundary conditions

The vascular tree grows under specific assumptions and boundary conditions.

The perfused volume is supposed convex and homogeneously filled. The terminal segments correspond to pre-arteriole level, feeding a non modeled micro-vasculature. The blood is an incompressible, homogeneous Newtonian fluid, studied in a steady state and in laminar flow conditions.

The resistance and the pressure drop of a segment j are defined by:

$$R_j = \frac{8\mu}{\pi}\frac{l_j}{r_j^4} \text{ with } \mu \text{ the viscosity} \tag{1}$$

$$\Delta P_j = R_j Q_j \tag{2}$$

The total resistance of the tree is calculated recursively by tree decomposition, considering parallel and serial arrangements.

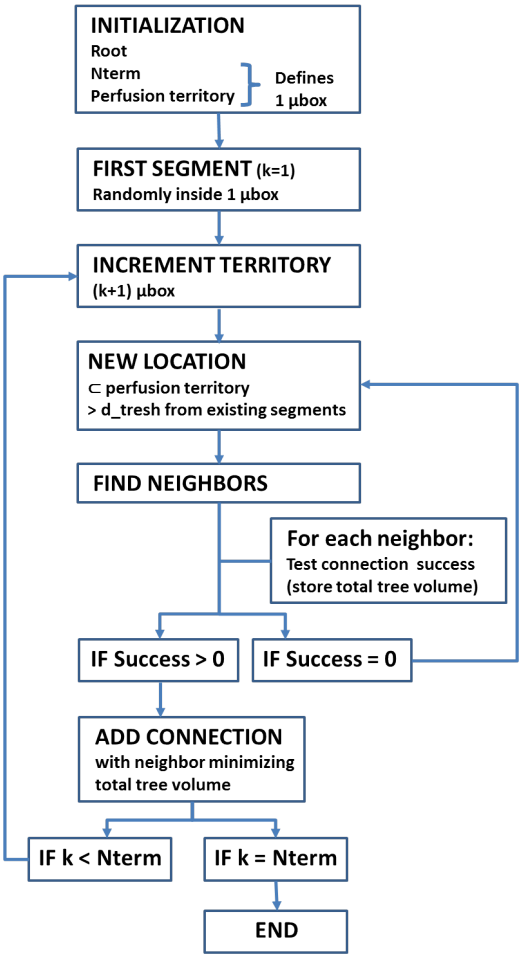

Figure 1: Algorithm of CCO. *d_tresh* is a distance threshold calculated at each iteration. A microbox corresponds to an average area per terminal segment.

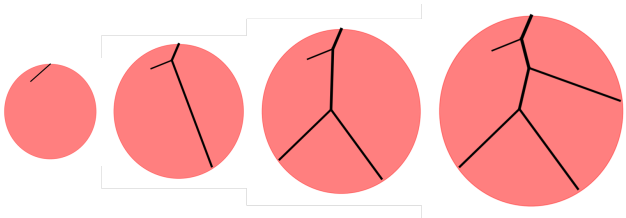

Figure 2: CCO example : output images of the first three loops.

Parameter	Meaning	Value
V_{perf}	perfusion volume	100 cm^3
P_{perf}	perfusion pressure	100 mmHg
P_{term}	terminal pressure	60 mmHg
Q_{perf}	perfusion flow	500 mL/ min
Q_{term}	terminal flow	0.125 mL/ min
N_{term}	number of terminals	4000
μ	viscosity of blood	3.6 cp
γ	Murray bifurcation exponent	3

Table 1: Global model parameters

The physiological parameters are set following table **??**:

The pressures at distal end of terminal segments, P_{term}, are equal and correspond to the inflow pressure to the micro-circulation.

The terminal flows $Q_{term,j}$ are equal, and delivered into the micro-circulation against P_{term}. Because of flow conservation, the $Q_{term,j}$ sum corresponds to the perfusion flow at the root Q_{perf}.

The laminar flow resistance of the whole tree induces a given total Q_{perf} accross the overall pressure drop ΔP.

The produced tree is binary and its total number of segments is calculated from:

$$N_{tot} = 2N_{term} - 1 \tag{3}$$

This tree is subjected to Murray's law, with a power coefficient equal to 3.

1.2 Initialization step

Inputs:

- convex perfusion surface (A_{perf}) or volume (V_{perf}) definition: position and shape. In our case we work within simple shapes: circular or spherical shape.
- number of terminal segments, N_{term}
- location of the root (in our case on the border of the perfusion territory)
- a random location inside the perfusion territory for the end of the first segment

From these inputs we estimate the average perfusion territory of each terminal segment when reaching the goal N_{term}, named "micro-circulatory black-box" [3]. We calculate r_{supp}, the average radius of the black-boxes:

$$\pi r_{supp}^2 = A_{perf} / N_{term} \tag{4}$$

Before adding a segment, the perfusion territory area is incremented of one micro-circulatory black-box. So, calling k_{term} the number of terminal segments at the current step of the algorithm, we obtain after the inflation the perfusion territory area A_k:

$$A_k = (k_{term} + 1)\pi r_{supp}^2 \tag{5}$$

The segments are stretched correspondingly to this inflation. First their new lengths are calculated, then each segment radius is rescaled in order to adapt the new tree resistance. Note that we do not recalculate segment positions after tree stretching but compute a conversion to the k_{world} via a scaling factor r_{kf}:

$$r_{kf} = \sqrt{\pi A_k} \tag{6}$$

The tree is adjusted to the inflated world before starting the loop to add a new segment.

In a similar fashion, knowing the flow at terminal segments Q_{term}, we will increase the perfusion flow with each during the loop to add a new segment, calculating as:

$$Q_{pk} = k_{term} Q_{term} \tag{7}$$

1.3 Loop to add new segment

We are provided a new location, n_{loc}, and want to find its optimal connection to the existing tree. For this purpose we select the N_{con} closest existing segments to this location, test their optimal connection to the new location, and store the total tree volume resulting of it. Then, as a global optimization process, we select the neighbor connection best minimizing the total tree volume.

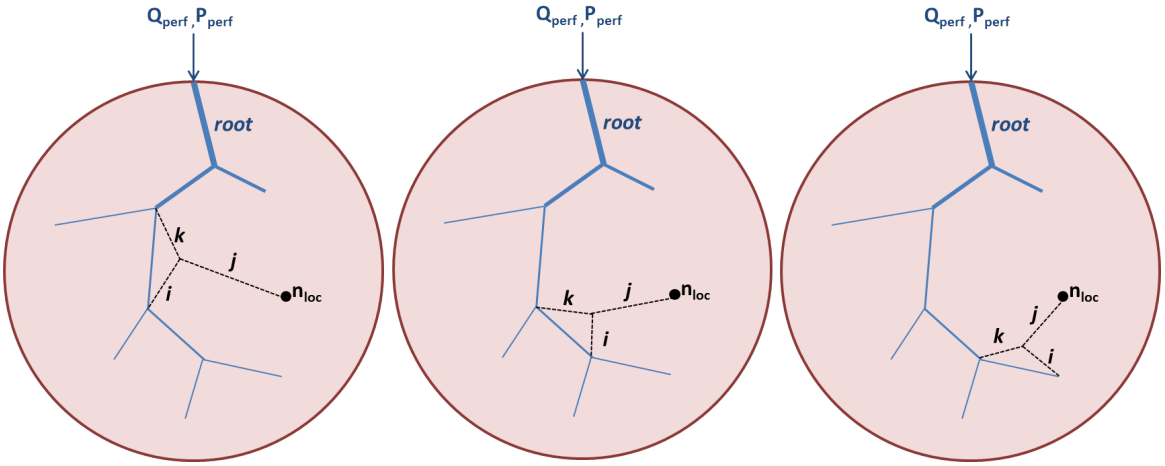

Figure 3: To add a new segment: test connection with neighbors of the new location n_{loc}

1.3.1 Constrained new location n_{loc}

A random position is picked, that has to fulfill two constraints: belonging to the perfusion territory and respecting a distance criterion. This criterion is defined based on the final and current size of the tree. In 2D, it is given by the following equation:

$$d_{thresh} = (\pi r_{supp}^2 / k_{term})^{\frac{1}{2}} \tag{8}$$

with r_{supp} calculated from equation (4).

In 3D this criterion is defined as:

$$d_{thresh} = (\frac{4}{3}\pi r_{supp}^3 / k_{term})^{\frac{1}{3}} \tag{9}$$

with

$$\frac{4}{3}\pi r_{supp}^3 = V_{perf} / N_{term} \tag{10}$$

This distance criteron is updated after each new segment is added, so that it decreases during tree growth. If no location is found (after $max\_trial = 1000$) that respects this distance to existing segments within the perfusion territory, then the distance criterion is multiplied by 0.9 and the process repeated until a new position is found that fulfills both constraints.

1.3.2 Test connection

The connection test corresponds to a single bifurcation optimization while taking into account its impact on the whole tree.

Kamiya proposes a single bifurcation optimization by an iterative procedure [2], which is fully detailed in section 2. At each of Kamiya's iteration, we are provided a bifurcation point location and radii of the concerned segments.

1. We control that the resulting segments are not degenerate, which means all three segments of the new bifurcations respect the following constraint between length and radius: $2r_i \leq l_i$. If they do degenerate we consider this bifurcation non plausible, skip it, and go to testing another neighbor segment.
2. We assess and apply the consequence of this connection on the whole tree before measuring the total tree volume. This process is detailed in sections 1.3.3 and 1.3.4.
3. We calculate the total tree volume gradient (relative to the previous result of Kamiya iteration). Along Kamiya's iterations, the total tree volume is expected to converge to a local minimum. The convergence is determined with a tolerance empirically fixed (in our case $tolerance = 0.01$).

If the convergence is reached, we apply an additional checks: we control that none of the three resulting segments overlap any other existing tree segment. The bifurcation location, segments radii, and total tree volume at convergence are stored to be later compared with other connections.

If the convergence has not been reached yet, we set the current radii and point location as a new starting point for Kamiya's optimization search.

1.3.3 Propagate new bifurcation impact on the whole tree

By adding a new terminal segment, generating a new bifurcation, we perturb the distribution of segmental flows. In order to reestablish the correct terminal flows, the hydrodynamic resistance of the tree must be adjusted. As the lengths of the segments as well as the terminal and perfusion pressures are fixed, this can only be accomplished by proper rescaling of the segment's radii.

If we define the reduced hydrodynamic resistance R^* as $R_i^* = R_i r_i^4$ we can calculate the reduced hydrodynamic resistance of a segment including its left and right subtrees by recursively traversing the subtrees:

$$R^*_{sub,j} = \frac{8\mu}{\pi} l_j + \left(\frac{(r_{left,j}/r_j)^4}{R^*_{left,j}} + \frac{(r_{right,j}/r_j)^4}{R^*_{right,j}} \right)^{-1} \tag{11}$$

Considering the equations (2) and (1), we can calculate the radius ratio of two children segments from resistance and flow:

$$\frac{r_i}{r_j} = \left(\frac{Q_i R^*_{sub,i}}{Q_j R^*_{sub,j}} \right)^{\frac{1}{4}} \tag{12}$$

with Q_i and Q_j the respective flow of sibling segments i and j.

Instead of storing the absolute radius for each segment, we consider the ratio between parent and its children: $\beta_k^i = r_i/r_k$ and $\beta_k^j = r_j/r_k$ with i and j the children, k the parent segment. Since the tree respects Murray's law, these ratios can actually be calculated directly from the ratio between children segments (see appendix A for details):

$$\beta_k^i = \left(1 + (\frac{r_i}{r_j})^{-\gamma} \right)^{-\frac{1}{\gamma}} \text{ and } \beta_k^j = \left(1 + (\frac{r_i}{r_j})^{\gamma} \right)^{-\frac{1}{\gamma}} \tag{13}$$

Calculating the reduced resistance for each children with (11), and knowing the flow, we obtain the children radius ratio from (12), which is used to calculate the β values, stored with the parent segment properties. The subtrees distal to the new bifurcation remain constant and unaffected by the addition of the new branch, whereas upstream bifurcations are updated following this exact same process. By this method, called "balancing of bifurcation ratios", radius rescaling is propagated up the tree.

1.3.4 Measure target function

Calculate the root radius from

$$r_{root} = \left(R^*_{sub,root} \frac{Q_{pk}}{P_{perf} - P_{term}} \right)^{\frac{1}{4}} \tag{14}$$

Then for each segment we obtain the radius from:

$$r_i = r_{root} \prod_{k=i}^{root} \beta_k \tag{15}$$

So we can calculate the total tree volume. This is the target function that we seek to minimize:

$$T_i = l_i^{\mu} r_i^{\lambda} \tag{16}$$

1.3.5 Select best connection between neighbors

We store the target function result in the Connection Evaluation Table (CET), for each of the tested neighbor connection. The connection yelding the lowest total tree volume is considered as the optimal one and added to the tree, updating flows and resistances.

If the CET does not contain at least two plausible connections among the $N_{con} = 20$ neighbors tested, then we extend the search to the $N_{max} = 40$ neighbor segments. If at least two plausible connections still do not come out of this process, we reject the tested location n_{loc} and start again the main loop to add a new segment with a new random location. By plausible connection we mean the local optimization converges, with no degenerate segment and no crossing of any other tree segment.

1.4 Example of results and comparison

When comparing image results of our simulated 4000 N_{term} tree, figure 4, with Schreiner's results [3],see figure 5, it seems we do not obtain the same radii.

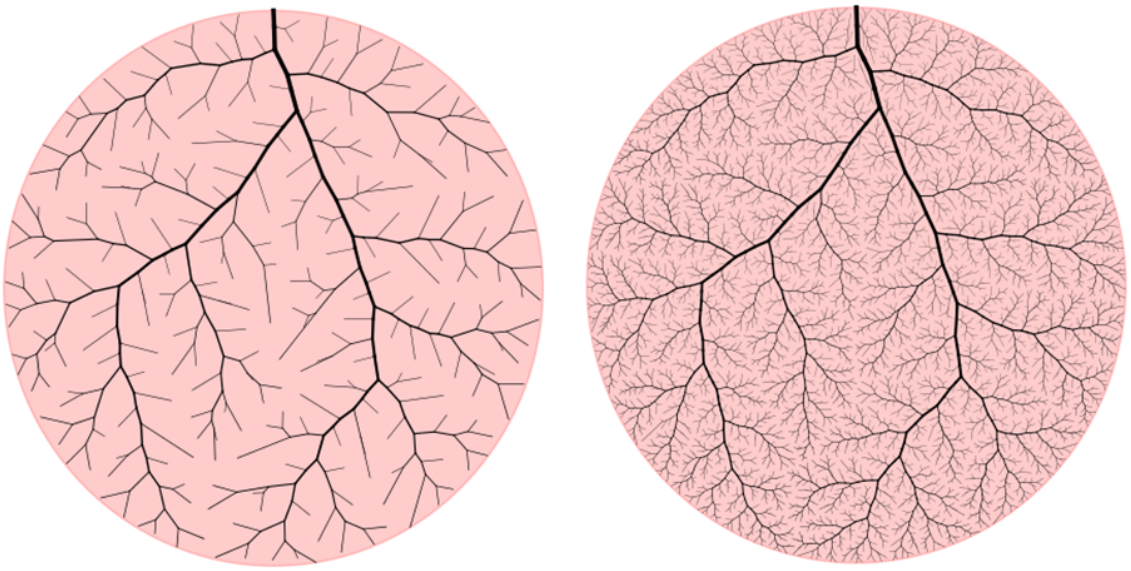

Figure 4: Output of CCO in 2D with different N_{Term}. (left) A $250N_{term}$ tree generated in 9 min. Note:The terminal pressure is adapted to the number of terminal segments, P_{term}=63 mmHg. (right) A $4000N_{term}$ tree generated in 33 hours.

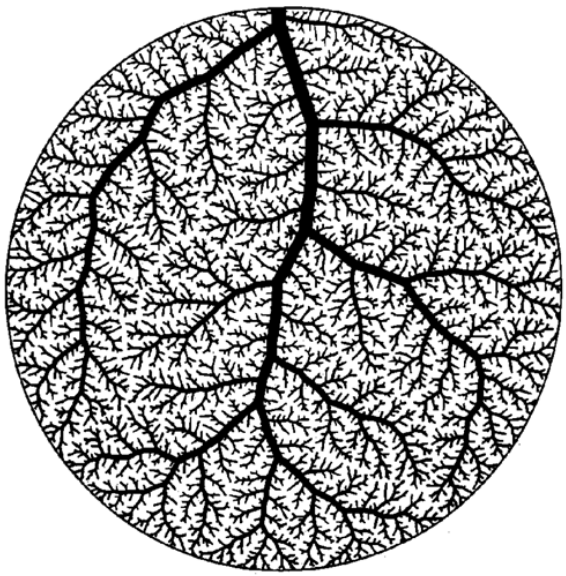

Figure 5: Fig 3 from Schreiner [3] : $4000N_{term}$ tree.

Actually, this visual difference might be due to their visualization tool resolution, that could be limited. Such assumption seems coherent when comparing the measured radii on $250N_{term}$ tree along bifurcation levels, cf figure 6.

Schreiner computed these 10 tree models with a Murray coefficient $\gamma = 2.55$. In figure 6 right, we provide the same study with different gamma values. Our curve for $\gamma = 2.55$ is pretty similar to Schreiner result, except that the slope is slightly steeper at the beginning. Also, our mean diameter tends to 0.5mm when reaching the 35th bifurcation level.

If we compare our 2D CCO radii distribution with Karch results (computed in 3D), in figure 7 we have similar mean variations, in particular the slope steepness along the first bifurcation levels.

The algorithm we implemented might not be exactly the same as Karch and Schreiner,due to internal parameters that were not detailed in their work, such as:

- *d_tresh* adaptation: we decrease *d_tresh* of 10% after 1000 unsuccessful iterations to get a new location inside perfusion territory far enough from existing segments. There are no precision, neither in Schreiner nor Karch work about this boundary.
- convergence boundary: we consider reaching convergence when total tree volume gradient between iterations is below 0.01 mm^3, and should be reached before 100 Kamiya's iterations.

Nonetheless, by comparing results, visually and quantitatively (radii study), we can assume we produced a similar CCO implementation.

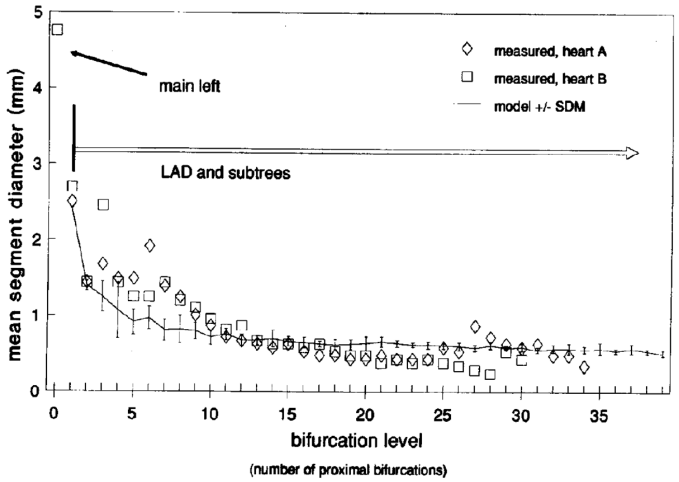

Fig. 4. Morphometric comparison between model and the left coronary artery trees of two humans. Vertical axis: averaged segment diameter. Horizontal axis: bifurcation level (= number of proximal bifurcations). Measurements from corrosion casts (1) of the left coronary circulation of two human hearts (symbols ◇ and □). Model simulations with 250 terminal branches (499 in total) refer to the LAD (or LCX) bed only and hence start at level 1 (polygon curve). Vertical bars represent standard deviations of means obtained from 10 model replicates with identical parameters (Table I), using different pseudo-random numbers, however. Computation time about 15 min per run.

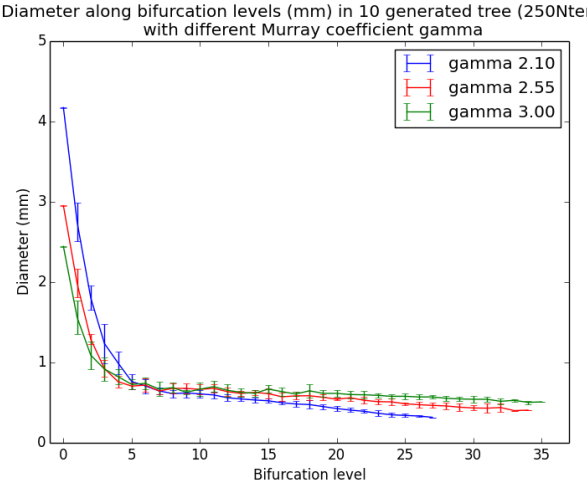

Figure 6: Radius study along bifurcation levels: mean and standard deviation at each bifurcation level on 10 simulated trees. Top: result from Schreiner [3], including simulated model and measured radii on anatomical data, computed with $\gamma = 2.55$. Bottom: our result comparing γ values: 2.1, 2.55 and 3.0.

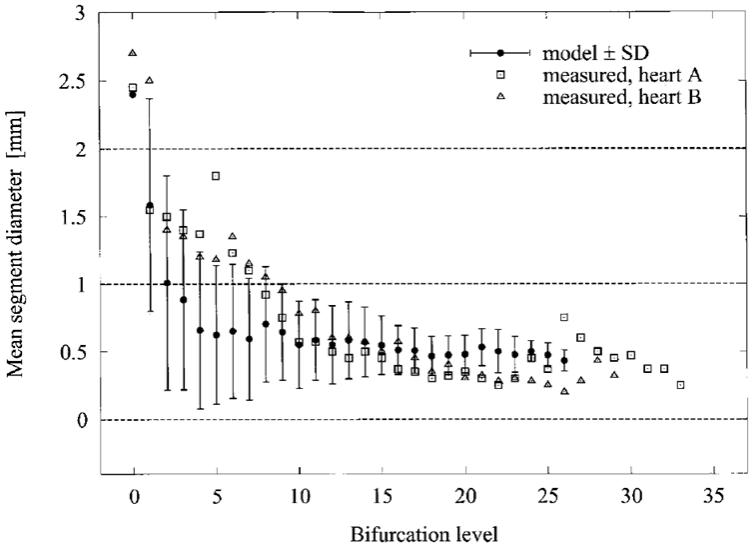

Fig. 6. Averaged segment diameters at respective bifurcation levels. Solid circles indicate the mean diameters of all vessel segments at a certain bifurcation level (defined as the number of proximal bifurcations). These data points were calculated from a CCO model tree with 250 terminal segments (499 segments in total) and with p_{term} set to 72 mm Hg. The remaining simulation parameters were identical to those used for Fig. 5 (cf. Table 1). Vertical bars represent standard deviations (S.D.) from the mean diameter values. Open squares and triangles denote measurements from corrosion casts of the coronary networks of two human hearts [39].

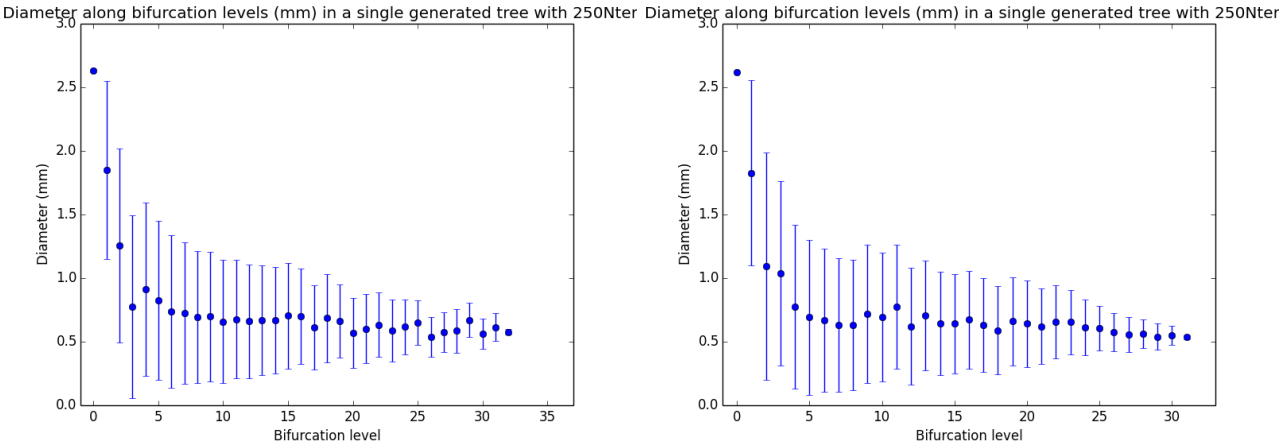

Figure 7: Radius study along bifurcation levels: mean and standard deviation at each bifurcation level on 1 single simulated 250Nterm tree. Top: result from Karch on 3D CCO [1], including simulated model and measured radii on anatomical data, computed with $\gamma = 3.0$. Bottom: our result computed on two trees from 2D CCO, with same γ value.

2 Local optimization: single bifurcation scale

Kamiya proposes a numerical solution to determine minimum volume bifurcation under restriction of physiological parameters, determinant pressure and flow, and locations of origin and terminals.

This method assumes the flow to be laminar and vessels are composed of straight ducts. In 2D the vessels are lying on a plane, whereas they are contained in a volume for the 3D implementation.

Note: Karch found that the optimum positions of the bifurcations in their 3D model trees were always found to lie in the plane defined by the endpoints of the respective three neighboring segments, which is consistent with the literature [4].

Process: iterative nested loops

Defining a starting position as the convex average of origin and terminal locations, weighted by respective flows.

$$(x, y) = (\frac{f_0 x_0 + f_1 x_1 + f_2 x_2}{2 f_0}, \frac{f_0 y_0 + f_1 y_1 + f_2 y_2)}{2 f_0}) \tag{17}$$

Calculate each segment length.

$$l_i^2 = (x - x_i)^2 + (y - y_i)^2 \tag{18}$$

Numerically calculate the new radii r_0, r_1,r_2. They are expected to satisfy both Hagen-Poiseuille's law and volume minimization.

When location of origin and two terminals segments, their pressure, and their flows are given, according to Hagen - Poiseuille's law:

$$\Delta P_1 = P_1 - P_0 = \kappa(\frac{f_0 l_0}{r_0^4} + \frac{f_1 l_1}{r_1^4}), \tag{19}$$

$$\Delta P_2 = P_2 - P_0 = \kappa(\frac{f_0 l_0}{r_0^4} + \frac{f_2 l_2}{r_2^4}) \tag{20}$$

Differentiating the tree volume with x, y and r_0 and equating them to zero, Kamiya obtains:

$$\frac{r_0^6}{f_0} = \frac{r_1^6}{f_1} + \frac{r_2^6}{f_2} \tag{21}$$

and

$$x = \frac{x_0 r_0^2/l_0 + x_1 r_1^2/l_1 + x_2 r_2^2/l_2}{r_0^2/l_0 + r_1^2/l_1 + r_2^2/l_2}, y = \frac{y_0 r_0^2/l_0 + y_1 r_1^2/l_1 + y_2 r_2^2/l_2}{r_0^2/l_0 + r_1^2/l_1 + r_2^2/l_2} \tag{22}$$

The details to get these equations is provided in appendix B.

Using $R = r^2$ in (21), we can express R_0 as:

$$R_0^3 = f_0(\frac{R_1^3}{f_1} + \frac{R_2^3}{f_2}) \tag{23}$$

Substituting this inside (20), one obtains the non linear system:

$$\begin{cases} \frac{\Delta P_1}{\kappa} R_1^2 \left(f_0 (\frac{R_1^3}{f_1} + \frac{R_2^3}{f_2}) \right)^{\frac{2}{3}} - f_0 l_0 R_1^2 - f_1 l_1 \left(f_0 (\frac{R_1^3}{f_1} + \frac{R_2^3}{f_2}) \right)^{\frac{2}{3}} = 0 \\ \frac{\Delta P_2}{\kappa} R_2^2 \left(f_0 (\frac{R_1^3}{f_1} + \frac{R_2^3}{f_2}) \right)^{\frac{2}{3}} - f_0 l_0 R_2^2 - f_2 l_2 \left(f_0 (\frac{R_1^3}{f_1} + \frac{R_2^3}{f_2}) \right)^{\frac{2}{3}} = 0 \end{cases} \tag{24}$$

We are looking for the root satisfying these equations using a non linear solver. If the solution converges, we get the new radii, that are needed to calculate the new position of the branching point in (22). This locations is a new input for the loop to iterate again (calculating length (18), then new radii (24), new location (22) and so on). If this iterative loop converges and the bifurcation total volume decreases, the equation system is solved and provides optimal radii and position for the bifurcation.

Note: in CCO the pressure is not determined all along vessels (only at the root and terminal segments). In order to adapt to our situation, we use an estimated radius to calculate the pressure drops using (20). At the first iteration the estimated radii are all equal to the segment's radius on which is connected the branch: $r_0 = r_1 = r_2 = r_{ori}$. Then, we will use the previously calculated radii to update the pressure drops at each iteration.

Example of results

We give examples of results on different type of bifurcations. For these examples we used a tolerance of 0.01 and maximum number of iteration of 100.

In the figure 8 (a), for symetric flows and child locations: the optimal bifurcation point corresponds to the convex average.

The figure 8 (b) illustrates well a Steiner solution to optimal network [5]: it is more advantageous to transport flows together by delaying bifurcation. In fluid mechanics context, this subadditivity follows from Poiseuille's law, according to which the resistance of a tube increases when it gets thinner.

The figure 8 (c) shows influence of blood demand on the bifurcation geometry: because flow is more important on the right child, the radius is bigger and the bifurcation is dragged toward this child. Also, we note that the bifurcation is less delayed than for symmetrical flows.

The figure 8 (d) shows the influence of both destination and demand.

Karch implementation

Karch added lower and upper bounds to Kamiya's algorithm that ensures: (1) the bifurcation position within the perfusion volume; (2) the non degeneracy of the bifurcation (by constraining segment length over segment diameter).

Conclusion

We implemented this CCO method with the same N_{con} and N_{max} as Karch (respectively 20 and 40). The 2D procedure is a good start for debugging, visualizing the results and should be easily convertible

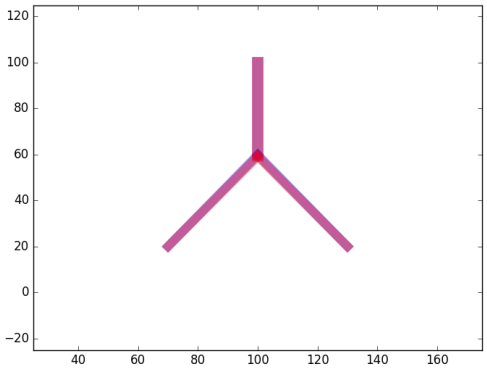

(a) $Q_l = Q_r = \frac{1}{2}Q_p$

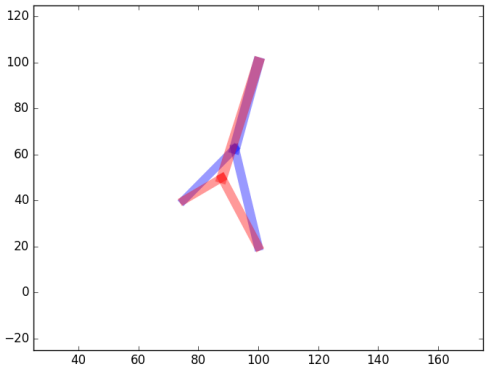

(b) Random child locations and $Q_l = Q_r = \frac{1}{2}Q_p$

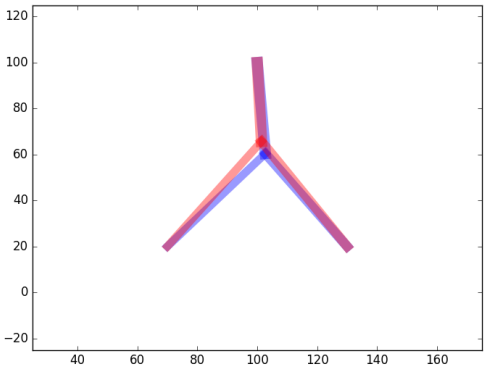

(c) $Q_l = \frac{1}{4}Q_p$ and $Q_l = \frac{3}{4}Q_p$

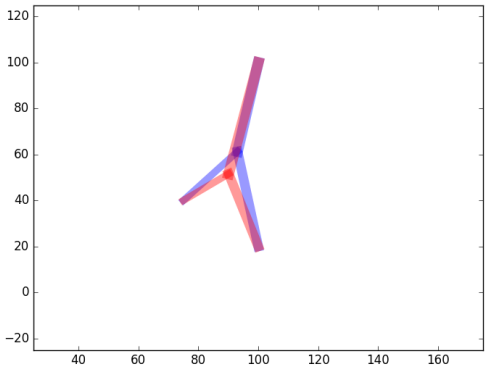

(d) Random child locations and $Q_l = \frac{1}{4}Q_p$, $Q_l = \frac{3}{4}Q_p$

Figure 8: In blue the starting bifurcation (convex average position), in red the final bifurcation after Kamiya's algorithm reached convergence (tolerance = 0.01). Convergence was reached at 15th, 24th, 31st and 21st iteration respectively in (a),(b),(c),(d). Q_p is the flow in parent branch, Q_l and Q_r are flows in left and right children.

into 3D CCO.

We improved computation time by parallelizing the connection test of neighbor segments. The code is available for 2D and 3D on git hub repo: `ClaraJaquet/HeartFlow/SyntheticTreeGeneration_Code`.

Appendices

A Equation (21), from Kamiya & Togawa 1972 equation (6)

Kamiya uses Murray definition at equation (7) from Physiological principle of minimum work [6] that he calls the simplest requirement for efficiency in the circulation:

$$f = kr^3$$

with k being a constant, so that the flow of blood past any section shall everywhere bear the same relation to the cube of the radius of the vessel at that point. Using it as:

$$r_i^3 = \frac{r_i^6 k}{f_i}$$

and combining it this with Murray's law,

$$r_0^\gamma = r_1^\gamma + r_2^\gamma \text{ with } \gamma = 3$$

where r_0 is the parent radius, r_1 and r_2 are the children radii, one obtains:

$$\frac{kr_0^6}{f_0} = \frac{kr_1^6}{f_1} + \frac{kr_2^6}{f_2}$$

that can be simplified into equation (21).

B Equation (22), from Kamiya & Togawa 1972 equation (7)

We have

$$V = \pi(r_0^2 l_0 + r_1^2 l_1 + r_2^2 l_2)$$

and

$$\begin{aligned} l_0^2 &= (x - x_0)^2 + (y - y_0)^2 \\ l_1^2 &= (x - x_1)^2 + (y - y_1)^2 \\ l_2^2 &= (x - x_2)^2 + (y - y_2)^2 \end{aligned}$$

We rewrite (B)

$$V = \pi(r_0^2\sqrt{(x - x_0)^2 + (y - y_0)^2} + r_1^2\sqrt{(x - x_1)^2 + (y - y_1)^2} + r_2^2\sqrt{(x - x_2)^2 + (y - y_2)^2})$$

We derive each term with respect to x.

$$\frac{\partial}{\partial x}\sqrt{(x-x_0)^2+(y-y_0)^2} = \frac{x-x_0}{\sqrt{(x-x_0)^2+(y-y_0)^2}} = \frac{x-x_0}{l_0},$$

same for the x_1 and x_2 term, so we have

$$\frac{\partial V}{\partial x} = \pi\left[\frac{r_0^2(x-x_0)}{l_0} + \frac{r_1^2(x-x_1)}{l_1} + \frac{r_2^2(x-x_2)}{l_2}\right] = 0$$

Discarding the π factor and separating the terms,

$$x\frac{r_0^2}{l_0} + x\frac{r_1^2}{l_1} + x\frac{r_2^2}{l_2} = x_0\frac{r_0^2}{l_0} + x_1\frac{r_1^2}{l_1} + x_2\frac{r_2^2}{l_2}$$
$$x(\frac{r_0^2}{l_0} + \frac{r_1^2}{l_1} + \frac{r_2^2}{l_2}) = x_0\frac{r_0^2}{l_0} + x_1\frac{r_1^2}{l_1} + x_2\frac{r_2^2}{l_2}$$

and thus

$$x = \frac{x_0\frac{r_0^2}{l_0} + x_1\frac{r_1^2}{l_1} + x_2\frac{r_2^2}{l_2}}{\frac{r_0^2}{l_0} + \frac{r_1^2}{l_1} + \frac{r_2^2}{l_2}}$$

This is one half of Eq.(7) in Kamiya & Togawa. The other half is obtained by substituting x with y everywhere. This is formally correct but not 100% satisfying since the l_i depend on x and y.

References

1. Rudolf Karch, Friederike Neumann, Martin Neumann, and Wolfgang Schreiner. A three-dimensional model for arterial tree representation, generated by constrained constructive optimization. *Computers in biology and medicine*, 29(1):19–38, 1999.
2. Akira Kamiya and Tatsuo Togawa. Optimal branching structure of the vascular tree. *The Bulletin of mathematical biophysics*, 34(4):431–438, 1972.
3. Wolfgang Schreiner and Peter Franz Buxbaum. Computer-optimization of vascular trees. *Biomedical Engineering, IEEE Transactions on*, 40(5):482–491, 1993.
4. M Zamir and H Chee. Branching characteristics of human coronary arteries. *Canadian journal of physiology and pharmacology*, 64(6):661–668, 1986.
5. Marc Bernot, Vicent Caselles, and Jean-Michel Morel. *Optimal transportation networks: models and theory*, volume 1955. Springer Science & Business Media, 2009.
6. Cecil D Murray. The physiological principle of minimum work i. the vascular system and the cost of blood volume. *Proceedings of the National Academy of Sciences*, 12(3):207–214, 1926.